



## Genome-wide evidence for speciation with gene flow in *Heliconius* butterflies

Simon H. Martin, Kanchon K. Dasmahapatra, Nicola J. Nadeau, et al.

*Genome Res.* 2013 23: 1817-1828 originally published online September 17, 2013

Access the most recent version at doi:[10.1101/gr.159426.113](https://doi.org/10.1101/gr.159426.113)

---

### Supplemental Material

<http://genome.cshlp.org/content/suppl/2013/09/17/gr.159426.113.DC1.html>

### References

This article cites 62 articles, 18 of which can be accessed free at:  
<http://genome.cshlp.org/content/23/11/1817.full.html#ref-list-1>

### Creative Commons License

This article is distributed exclusively by Cold Spring Harbor Laboratory Press for the first six months after the full-issue publication date (see <http://genome.cshlp.org/site/misc/terms.xhtml>). After six months, it is available under a Creative Commons License (Attribution-NonCommercial 3.0 Unported), as described at <http://creativecommons.org/licenses/by-nc/3.0/>.

### Email Alerting Service

Receive free email alerts when new articles cite this article - sign up in the box at the top right corner of the article or [click here](#).

---

---

To subscribe to *Genome Research* go to:  
<http://genome.cshlp.org/subscriptions>

---

# Genome-wide evidence for speciation with gene flow in *Heliconius* butterflies

Simon H. Martin,<sup>1,8</sup> Kanchon K. Dasmahapatra,<sup>2,3</sup> Nicola J. Nadeau,<sup>1</sup> Camilo Salazar,<sup>4</sup> James R. Walters,<sup>5</sup> Fraser Simpson,<sup>2</sup> Mark Blaxter,<sup>6</sup> Andrea Manica,<sup>1</sup> James Mallet,<sup>2,7</sup> and Chris D. Jiggins<sup>1</sup>

<sup>1</sup>Department of Zoology, University of Cambridge, Cambridge CB2 3EJ, United Kingdom; <sup>2</sup>Department of Genetics, Evolution and Environment, University College London, London WC1E 6BT, United Kingdom; <sup>3</sup>Department of Biology, University of York, York YO10 5DD, United Kingdom; <sup>4</sup>Facultad de Ciencias Naturales y Matematicas, Universidad del Rosario, Bogota DC, Colombia; <sup>5</sup>Department of Biology, Stanford University, Stanford, California 94305, USA; <sup>6</sup>Institute of Evolutionary Biology, The University of Edinburgh, Edinburgh EH9 3JT, United Kingdom; <sup>7</sup>Department of Organismic and Evolutionary Biology, Harvard University, Cambridge, Massachusetts 02138, USA

Most speciation events probably occur gradually, without complete and immediate reproductive isolation, but the full extent of gene flow between diverging species has rarely been characterized on a genome-wide scale. Documenting the extent and timing of admixture between diverging species can clarify the role of geographic isolation in speciation. Here we use new methodology to quantify admixture at different stages of divergence in *Heliconius* butterflies, based on whole-genome sequences of 31 individuals. Comparisons between sympatric and allopatric populations of *H. melpomene*, *H. cydno*, and *H. timareta* revealed a genome-wide trend of increased shared variation in sympatry, indicative of pervasive interspecific gene flow. Up to 40% of 100-kb genomic windows clustered by geography rather than by species, demonstrating that a very substantial fraction of the genome has been shared between sympatric species. Analyses of genetic variation shared over different time intervals suggested that admixture between these species has continued since early in speciation. Alleles shared between species during recent time intervals displayed higher levels of linkage disequilibrium than those shared over longer time intervals, suggesting that this admixture took place at multiple points during divergence and is probably ongoing. The signal of admixture was significantly reduced around loci controlling divergent wing patterns, as well as throughout the Z chromosome, consistent with strong selection for Müllerian mimicry and with known Z-linked hybrid incompatibility. Overall these results show that species divergence can occur in the face of persistent and genome-wide admixture over long periods of time.

[Supplemental material is available for this article.]

Ongoing hybridization between closely related species appears to be common in nature (Mallet 2005; Rieseberg 2009) and theoretical work has demonstrated a diversity of scenarios whereby species can emerge without complete geographical isolation (Kirkpatrick and Ravigné 2002; Gavrillets 2004; van Doorn et al. 2009). Despite widespread interest in these scenarios, there remains little consensus among speciation biologists regarding the extent to which ongoing gene flow actually plays a role during speciation. This is partly because it is challenging to reconstruct ancestral ranges and therefore almost impossible to know for sure the extent of historical contact between species. Fortunately, genomic approaches are now beginning to allow us to address these long-standing questions from a different angle, by documenting the extent of admixture between species on a genome-wide scale (Kulathinal et al. 2009; Ellegren et al. 2012; Garrigan et al. 2012; The *Heliconius* Genome Consortium 2012; Nosil et al. 2012). Speciation genomics therefore offers an opportunity to address long-standing questions regarding the extent to which divergence and speciation occurs in the face of ongoing gene flow.

One prediction of models of speciation with gene flow is that the level of divergence should be heterogeneous across the genome. Some loci are likely to be shared between incipient species, while selection maintains divergence at others (Turner et al. 2005; Nosil et al. 2009). Recently, considerable progress has been made in documenting patterns of genomic divergence between incipient species (Hohenlohe et al. 2010; Lawnczak et al. 2010; Michel et al. 2010; Ellegren et al. 2012; Nosil et al. 2012; Gagnaire et al. 2013). Genome-wide studies of threespine sticklebacks (Hohenlohe et al. 2010, 2012) and *Ficedula* flycatchers (Ellegren et al. 2012) revealed patterns of divergence consistent with a model of “islands” of divergence amidst a sea of gene flow. In contrast, analyses of *Anopheles gambiae* subspecies (Lawnczak et al. 2010) and *Rhagoletis* host races (Michel et al. 2010) reported widespread divergence throughout the genome. One problem is that patterns of divergence are typically noisy, reflecting the complex interactions of selection, drift, migration, recombination, mutation, and ancestral polymorphism, all of which can lead to heterogeneity in divergence

**\*Corresponding author**  
E-mail [shm45@cam.ac.uk](mailto:shm45@cam.ac.uk)

Article published online before print. Article, supplemental material, and publication date are at <http://www.genome.org/cgi/doi/10.1101/gr.159426.113>.

© 2013 Martin et al. This article is distributed exclusively by Cold Spring Harbor Laboratory Press for the first six months after the full-issue publication date (see <http://genome.cshlp.org/site/misc/terms.xhtml>). After six months, it is available under a Creative Commons License (Attribution-NonCommercial 3.0 Unported), as described at <http://creativecommons.org/licenses/by-nc/3.0/>.

(Noor and Bennett 2009; Michel et al. 2010; Nadeau et al. 2012). A key challenge is therefore to distinguish the signal of gene flow from background noise.

Analyses of genomic divergence therefore need to be complemented with more sensitive tests for gene flow between populations (Kulathinal et al. 2009; Ellegren et al. 2012; Garrigan et al. 2012; The *Heliconius* Genome Consortium 2012; Nosil et al. 2012). A widely used approach is to fit coalescent models (Pinho and Hey 2010), but this can be computationally prohibitive for genomic data sets and requires strong assumptions about population parameters. A simpler method is to compare the extent of shared variation between sympatric and allopatric populations (Grant et al. 2005). Recent gene flow should result in reduced differentiation and an excess of shared variation between sympatric populations compared with allopatric populations. This logic has been applied on a genomic scale to test for gene flow in *Drosophila* (Kulathinal et al. 2009) and hominids (Green et al. 2010). However, this approach does not account for the age of shared variation, such that recent admixture may be confounded with ancestral geographic structure (Green et al. 2010; Durand et al. 2011; Eriksson and Manica 2012). It is therefore best used in combination with other methods that can distinguish recent gene flow from ancient shared variation.

In this paper, we focus on the closely related neotropical butterfly species *Heliconius melpomene*, *Heliconius cydno*, and *Heliconius timareta* (Fig. 1). These species are distasteful to predators and often involved in Müllerian mimicry with other species. All three comprise multiple distinct wing pattern races that have been

considered as an early stage in speciation (Jiggins 2008). Indeed there is strong evidence that selection for Müllerian mimicry can lead to wing pattern divergence and assortative mating without the need for geographic separation (Chamberlain et al. 2009). *Heliconius cydno* and *H. timareta* together form a clade that is sister to *H. melpomene*, estimated about two million years divergent (Bull et al. 2006; Salazar et al. 2008). *Heliconius melpomene* and *H. cydno* have distinct wing patterns and other ecological differences, and display strong assortative mating (Merrill et al. 2011a). Hybrids occur at low frequency (<1/1000) (Mallet et al. 2007), and are female-sterile (Naisbit et al. 2002), as well as being preferentially attacked by predators due to their non-mimetic wing patterns (Merrill et al. 2012). Unlike *H. cydno*, several *H. timareta* races have *H. melpomene*-like patterns (Giraldo et al. 2008; Mérot et al. 2013) and similarly show differences in host plant use and mating preferences (Giraldo et al. 2008). Recent genomic studies have begun to dissect the genetic variation underlying color pattern diversity in this genus (The *Heliconius* Genome Consortium 2012; Nadeau et al. 2012; Supple et al. 2013). One important insight is that the shared color patterns between *H. melpomene* and *H. timareta* appear to have resulted from introgression (The *Heliconius* Genome Consortium 2012; Pardo-Díaz et al. 2012). There is also evidence for exchange of other loci between *H. melpomene* and the *H. cydno/timareta* clade (Bull et al. 2006; Kronforst et al. 2006; The *Heliconius* Genome Consortium 2012; Pardo-Díaz et al. 2012; Nadeau et al. 2013). RAD-tag analyses of Peruvian races of *H. melpomene* and *H. timareta* suggest that at least ~2%–5% of the genome is admixed (The *Heliconius* Genome Consortium 2012). The recent completion of the *H. melpomene* genome now allows investigation of genome-wide patterns of divergence and gene flow within and between these species.

Here we take advantage of the geographic distribution of *H. melpomene*, with some populations many thousands of kilometers from the current range of the *H. cydno/timareta* clade (Fig. 1), and carry out a much more powerful genome-wide test for gene flow than was possible with the sequenced fragments hitherto studied. We analyzed 31 resequenced individuals (30 of which were newly sequenced in this study) from replicate sympatric species pairs of the two clades in Peru, where they are convergent in wing pattern, and Panama, where they are divergent. We also sampled an allopatric *H. melpomene* population from French Guiana (Fig. 1). Four species of the silvaniform clade of *Heliconius* were included as outgroups. Our new methods allowed us to investigate the extent and time course of genomic admixture, both before speciation and during different time periods after speciation.

## Results

### Phylogenomic analysis

Five populations of *H. melpomene*, one population of *H. cydno*, one population of *H. timareta*, and four outgroup species were sequenced (Fig. 1; Supplemental Table S1). Populations were represented by four wild-caught individuals (eight haploid genomes) except *H. m. melpomene* from Panama, for which three individuals were sampled (Supplemental Table S1). All individuals were wild-caught except for *H. m. melpomene* specimen no. 1, which was from the inbred reference genome strain. Whole-genome shotgun sequencing using the Illumina GA IIx and HiSeq 2000 technology gave an average coverage per individual of 15–62× (Supplemental Table S1). Sequences were aligned to the *H. melpomene* reference genome (The *Heliconius* Genome Consortium 2012) (version 1.1),

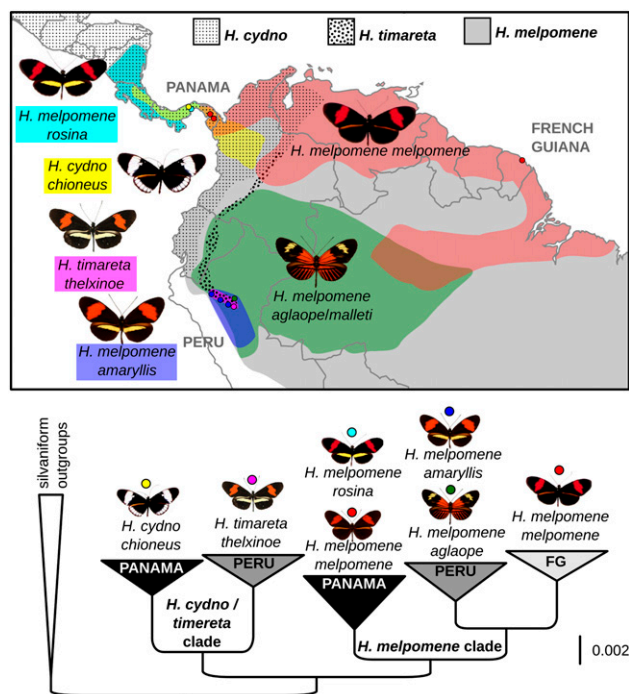


**Figure 1.** Populations sampled and their phylogenetic relationships. The entire distribution of *H. melpomene* is shown in gray. The entire distribution of the *H. cydno/timareta* clade is shown with dots (Rosser et al. 2012). Colors depict distributions of races used in this study, with dots indicating the sampling locations, and correspond to the colored dots on the tree. The tree is a compressed version of the whole-genome ML tree (Supplemental Fig. S1). The three general sampling locations, Panama, Peru, and French Guiana, are indicated. The scale bar refers to the number of substitutions per site.

including the complete mitochondrial scaffold. Genotyping and quality filtering (see Methods for details) produced an average of 190 million high-quality genotype calls per individual (69% of the genome). Proportions of variant sites were similar across all wild-caught individuals, and the ratio of transitions to transversions with respect to the reference was similar across all taxa, indicating that there was no systematic bias in the distribution of sequencing errors among taxa.

Maximum likelihood (ML) phylogenetic reconstruction using all sites with high-quality genotype calls for all 31 individuals (60 Mb of sequence, ~25% of the genome) confirmed that the *H. melpomene* and the *H. cydno/timareta* clades are reciprocally monophyletic (Fig. 1; Supplemental Fig. S1; The *Heliconius* Genome Consortium 2012; Nadeau et al. 2013). We here term this topology “the species tree.” A tree generated from complete mitochondrial sequences produced a similar topology (Supplemental Fig. S1).

### Phylogenetic discordance across the genome

Although the genome-wide ML tree revealed strong support for the expected “species tree,” most speciation scenarios predict discordant coalescent histories among genomic regions (Garigan et al. 2012). To investigate this, we generated maximum-likelihood trees for non-overlapping 100-kb windows throughout the genome. To simplify the hypotheses being tested, we analyzed two sets of four taxa separately, each representing a sympatric species pair and an allopatric “control” population. The *cydno/melpomene* set consisted of *H. cydno* and *H. m. rosina* (both from Panama), *H. m. melpomene* from French Guiana and outgroups, while the *timareta/melpomene* set consisted of *H. timareta* and *H. m. amaryllis* (both from Peru), with *H. m. melpomene* from French Guiana and outgroups. We summed the frequency of four possible topologies: species, geography, control, and unresolved (Fig. 2B). Three of these we considered “resolved,” meaning that two of the ingroup populations (eight individuals) formed a monophyletic clade, while the four individuals comprising the third ingroup population formed a distinct monophyletic sister clade (see Supplemental Fig. S3 for examples). For both data sets, the majority of genomic windows (53% and 53.2%, respectively) supported a resolved “species tree” topology in which the *H. melpomene* populations are monophyletic (Fig. 2). Under a bifurcating topology, incomplete lineage sorting should result in similar numbers of two alternative resolved topologies, which we term the “geography tree” (sympatric populations of different species cluster together) and the “control tree” (allopatric populations of different species cluster together). The final

possibility is an “unresolved tree,” in which the three ingroup populations are not neatly partitioned into two monophyletic clusters (Fig. 2; see Supplemental Fig. S3 for examples).

As expected under admixture, we found that the geography tree was far more prevalent than the control tree in both data sets: 42.2% versus 1.1% for the *cydno/melpomene* set and 18.5% versus 2.7% for the *timareta/melpomene* set; and widely distributed across the genome (Fig. 2C; Supplemental Fig. S4). While only 3.7% of trees were unresolved in the *cydno/melpomene* set, 25.6% were unresolved in the *timareta/melpomene* set. The greater fraction of unresolved trees in the second case is expected given greater shared ancestral polymorphism due to the more recent divergence between *H. m. amaryllis* and *H. m. melpomene* from French Guiana (Fig. 1; Supplemental Fig. S1). These findings show that there is not only a large amount of phylogenetic discordance across the genome, but that it is strongly structured by geography, consistent with gene flow between these clades where their ranges overlap.

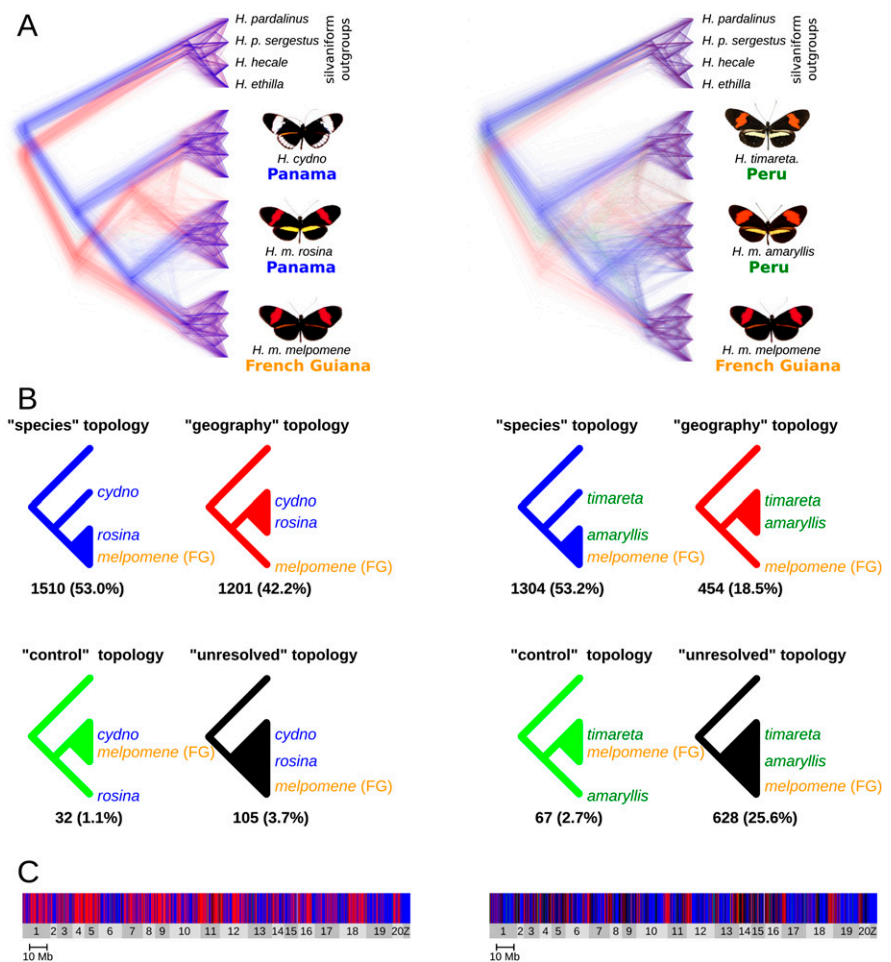


**Figure 2.** Four-taxon ML trees for 100-kb windows. (A) Trees were superimposed using DensiTree (Bouckaert 2010). There were 2848 trees for the *H. cydno*–*H. melpomene* data set (left) and 2453 for the *H. timareta*–*H. melpomene* data set (right). Tree lengths were equalized so that all trees could be superimposed, and then a random jitter was added to all branch lengths to show density. Trees supporting each of the four possible topologies are colored accordingly: blue for the species tree, red for the geography tree, green for the control tree, and black for unresolved trees. (B) The four topologies scored, along with the number and percentage of trees supporting each. See Supplemental Figure S3 for examples of trees assigned to each topology. (C) The distribution of the four topologies across the genome. Chromosomes are shaded light and dark gray. See Supplemental Figure S4 for an enlarged version.

Here we report results for 100-kb windows because linkage disequilibrium (LD) tends to break down completely within 100 kb in *Heliconius* genomes (Supplemental Fig. S2), making each 100-kb block effectively independent from its neighbors. However, we also repeated the tests at various window sizes between 10 and 200 kb (Supplemental Table S2). Although the number of unresolved trees increases at smaller window sizes, the relative ratios of resolved trees are robust to window size variation (Supplemental Table S2).

### Evidence of recent gene flow

Allele frequency correlations provide further evidence for recent interspecific gene flow. Our geographically structured sampling design allowed us to distinguish between ancient and recent admixture using a sensitive “four-population” test (Reich et al. 2009, 2012) for geographical correlations in allele frequencies. In the absence of admixture, allele frequency changes due to drift in disparate populations should not be correlated. Across all tests, there was a highly significant allele frequency correlation between *H. m. rosina* and *H. cydno* from Panama, and between *H. m. amaryllis* and *H. timareta* from Peru (Table 1). These correlations indicate recent gene flow between these species where they occur in sympatry.

### Gene flow has occurred at multiple points since early in speciation

Evidence for recent gene flow does not necessarily imply that gene flow has persisted throughout speciation. Secondary contact after allopatric speciation might be characterized by a burst of recent gene flow, while sympatric speciation should leave a signature of continuous gene flow during speciation. We estimated admixture along different branches of the phylogeny using a method devised by Green et al. (2010), which compares two classes of shared derived alleles, termed ABBA and BABAs. For three populations and an outgroup, with the relationship  $[(P_1, P_2), P_3], O$ , we can test for differential admixture between  $P_3$  and either of  $P_1$  or  $P_2$  by examining the numbers of shared derived alleles between  $P_3$  and  $P_2$  (ABBAs) and between  $P_3$  and  $P_1$  (BABAs). We calculated two sta-

tistics: “ $D$ ” used to test for a significant imbalance of ABBA and BABAs, indicative of admixture; and “ $f$ ,” the estimated fraction of the genome that has been shared between populations (Green et al. 2010; Durand et al. 2011). These measures are robust to variation in effective population size (Durand et al. 2011).

We examined rates of gene flow between *H. timareta* and *H. m. amaryllis* across three time periods (Fig. 3): a short, recent period, subsequent to the divergence between *H. m. amaryllis* and *H. m. aglaope* (period 4 of Fig. 3A); an intermediate period, subsequent to the divergence of the Peruvian populations from French Guianan *H. m. melpomene* (periods 3, 4 of Fig. 3A); and a long period, subsequent to the divergence between Peruvian and Panamanian populations (periods 2, 3, 4 of Fig. 3A). Across these comparisons there was a strong trend of increasing  $f$  with time (Fig. 3C; Table 2). Similarly, for *H. m. rosina* and *H. cydno*, over two time periods,  $f$  was again much greater for the longer period (Fig. 3C; Table 2). Because this method assumes unidirectional gene flow from  $P_3$ , and complete isolation between  $P_3$  and  $P_1$ , the actual fraction of the genome that has been shared may be greater than estimated here. What is important is that the relative values of  $f$  increase with the length of the period examined, which is consistent with gene flow having occurred during time periods 2, 3, and 4. One potential caveat is that the extent of isolation between  $P_3$  and  $P_1$  could differ between these tests, accounting for some of the variation in  $f$ . We therefore investigated linkage disequilibrium among these shared derived sites as an additional signal to differentiate between recent and long-term gene flow.

### Linkage disequilibrium between shared derived alleles

The extent of LD between introgressed alleles carries information about the age of admixture. Recently introgressed haplotypes have had insufficient time to be broken down by recombination, and therefore closely linked introgressed alleles should occur in LD with one another (Machado et al. 2002; Sankararaman et al. 2012). In contrast, anciently introgressed alleles should display levels of LD similar to the average genomic level. We tested for this signal by examining LD at sites carrying shared derived variants (i.e., ABBA SNPs) in *H. m. amaryllis* and *H. m. rosina*. For *H. m. amaryllis*, three sets of SNPs carrying shared variants could be examined, corresponding to the three time periods described above (Fig. 3B). Likewise, in *H. m. rosina*, two sets of SNPs could be examined.

We found that the extent of LD differed dramatically between the time periods (Fig. 3D). Variants shared between *H. timareta* and *H. m. amaryllis* but absent from *H. m. aglaope* displayed the strongest LD, extending up to a megabase. This is consistent with the existence of large introgressed haplotypes that have yet to be fully broken down. Variants shared between *H. timareta* and *H. m. amaryllis* but absent from French Guianan *H. m. melpomene* displayed weaker LD, while those shared between *H. timareta* and *H. m. amaryllis* but absent from *H. m. rosina* displayed the weakest LD, declining with distance at a similar rate to the genomic average (Fig. 3D). Thus, these two latter comparisons include variation that ap-

**Table 1.** Results of the four-population test for recent gene flow

Test <sup>a</sup>	$f_4 \pm \text{std err}$	Z-score	P-value
Whole genome			
$f_4(\text{cydno}, \text{timareta}; \text{rosina}, \text{melp. [FG]})$	$0.0764 \pm 0.0013$	$60.14^b$	$<0.0001$
$f_4(\text{cydno}, \text{timareta}; \text{amaryllis}, \text{melp. [FG]})$	$-0.0370 \pm 0.0016$	$-22.70^b$	$<0.0001$
$f_4(\text{cydno}, \text{timareta}; \text{rosina}, \text{melp. [Pan]})$	$0.0056 \pm 0.0005$	$10.95^b$	$<0.0001$
$f_4(\text{cydno}, \text{timareta}; \text{amaryllis}, \text{aglaope})$	$-0.0039 \pm 0.0006$	$-6.91^b$	$<0.0001$
$f_4(\text{cydno}, \text{timareta}; \text{rosina}, \text{amaryllis})$	$0.0883 \pm 0.0015$	$58.51^b$	$<0.0001$
Z chromosome			
$f_4(\text{cydno}, \text{timareta}; \text{rosina}, \text{melp. [FG]})$	$0.0256 \pm 0.0064$	$4.00^c$	$0.0001$
$f_4(\text{cydno}, \text{timareta}; \text{amaryllis}, \text{melp. [FG]})$	$-0.0235 \pm 0.0100$	$-2.34^d$	$0.0192$
$f_4(\text{cydno}, \text{timareta}; \text{rosina}, \text{melp. [Pan]})$	$0.0021 \pm 0.0027$	$0.77$	$0.4418$
$f_4(\text{cydno}, \text{timareta}; \text{amaryllis}, \text{aglaope})$	$-0.0108 \pm 0.0104$	$-1.04$	$0.2997$
$f_4(\text{cydno}, \text{timareta}; \text{rosina}, \text{amaryllis})$	$0.0394 \pm 0.0085$	$4.64^b$	$<0.0001$

(aglaope) *H. m. aglaope*; (amaryllis) *H. m. amaryllis*; (rosina) *H. m. rosina*; (melp.) *H. m. melpomene*; (cydno) *H. c. chioneus*; (timareta) *H. t. thelxinoe*; (Pan) Panama; (FG) French Guiana.

<sup>a</sup>For  $f_4(A, B; C, D)$ , a significantly positive Z-score implies gene flow between A and C, or B and D, or both. A significantly negative Z-score implies gene flow between A and D, or B and C, or both.

<sup>b</sup>Indicates  $f_4$  significantly different from 0,  $P < 0.0001$ .

<sup>c</sup>Indicates  $f_4$  significantly different from 0,  $P < 0.01$ .

<sup>d</sup>Indicates  $f_4$  significantly different from 0,  $P < 0.05$ .

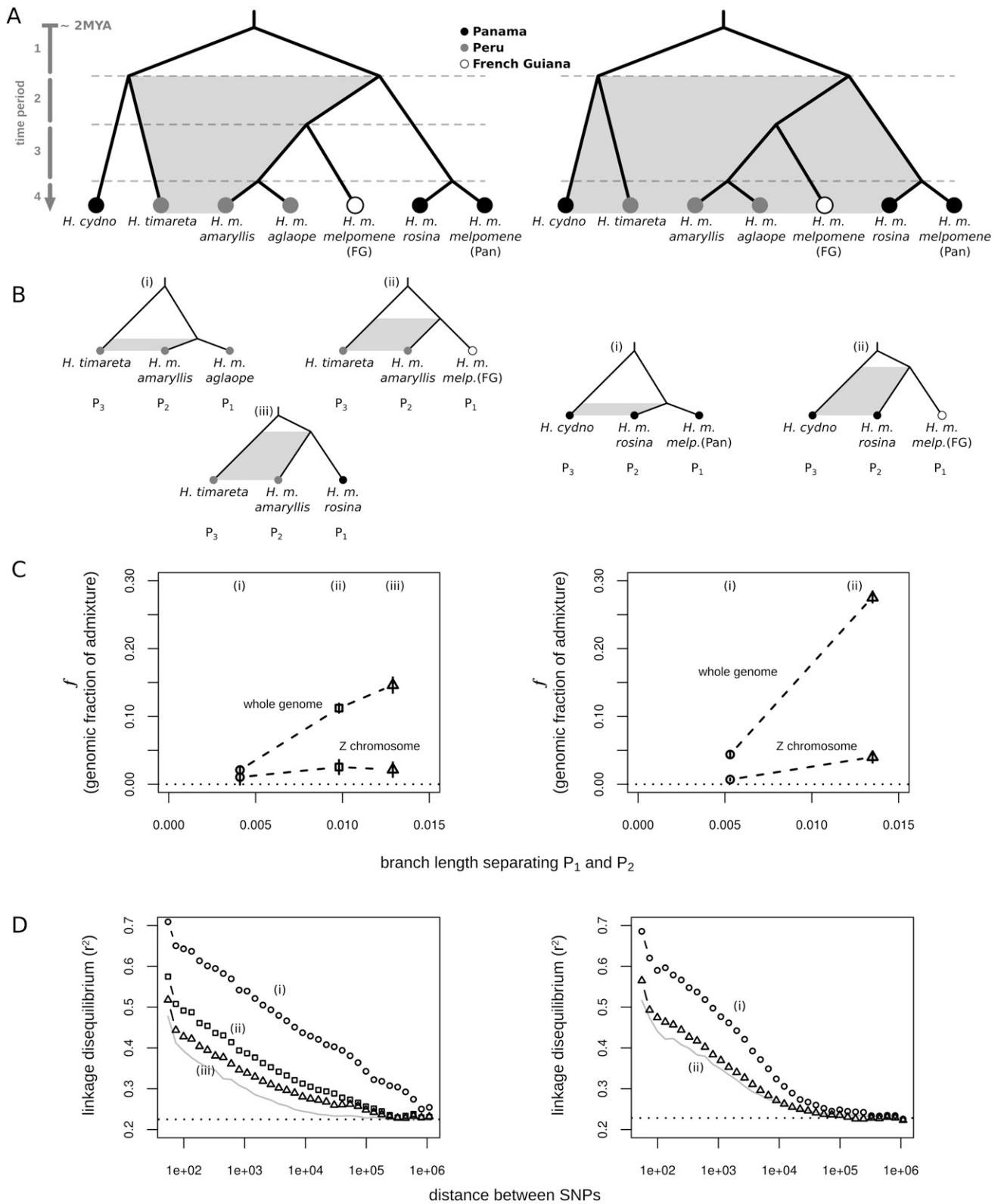


**Figure 3.** Measuring admixture at different phylogenetic scales. (A) We can distinguish between admixture in different time periods as follows. If gene flow was ancient only (i.e., period 1), then *H. m. amaryllis* and *H. m. rosina* should both be equally admixed with *H. timareta* and *H. cydno*. However, if gene flow is more recent (i.e., period 2, 3, or 4), then *H. m. amaryllis* should be more admixed with Peruvian *H. timareta*, and *H. m. rosina* should be more admixed with Panamanian *H. cydno*. The same logic applies when quantifying admixture for a specific branch: If *H. timareta* shares more derived alleles with *H. m. amaryllis* than with *H. m. aglaope*, this skew must reflect gene flow between *H. timareta* and *H. m. amaryllis* that is more recent than the coalescence between *H. m. amaryllis* and *H. m. aglaope* (i.e., during period 4). (B) Our sampling allowed us to quantify admixture at three time scales between *H. timareta* and *H. m. amaryllis*, and two time scales between *H. cydno* and *H. m. rosina*. (C) The estimated fraction of admixture ( $f$ ), plotted for the whole genome and the Z chromosome specifically against the estimated length of the time period being analyzed, calculated as the average branch length separating populations P<sub>1</sub> and P<sub>2</sub> in the genomic ML phylogeny (Supplemental Fig. S1). Vertical lines depict standard errors. (D) LD ( $r^2$ ) between shared-derived alleles in the P<sub>2</sub> population (left, *H. m. amaryllis*; right, *H. m. rosina*), plotted as a function of distance on a logarithmic scale. The SNPs used to estimate LD were those carrying a shared derived allele in P<sub>2</sub> and P<sub>3</sub>, while P<sub>1</sub> was fixed for the ancestral state (i.e., an ABBA pattern, where the B alleles are not necessarily fixed). The gray line represents the average genomic LD level, and the dashed line shows the average LD among unlinked sites.



**Table 2.** Results of ABBA BABA tests to quantify gene flow over specific time periods

P <sub>1</sub>	P <sub>2</sub>	P <sub>3</sub>	Time period <sup>a</sup>	D <sup>b</sup>	Z <sup>c</sup>	P-value <sup>c</sup>	f (%) <sup>d</sup>
Whole genome							
<i>aglaope</i>	<i>amaryllis</i>	<i>timareta</i>	4	0.039 ± 0.006	6.58 <sup>e</sup>	<0.0001	2.1 ± 0.3
<i>melp.</i> (FG)	<i>amaryllis</i>	<i>timareta</i>	4 + 3	0.197 ± 0.009	22.60 <sup>e</sup>	<0.0001	11.2 ± 0.7
<i>rosina</i>	<i>amaryllis</i>	<i>timareta</i>	4 + 3 + 2	0.209 ± 0.013	16.09 <sup>e</sup>	<0.0001	14.6 ± 1.2
<i>melp.</i> (Pan)	<i>amaryllis</i>	<i>timareta</i>	4 + 3 + 2	0.229 ± 0.013	17.38 <sup>e</sup>	<0.0001	15.6 ± 1.2
<i>melp.</i> (Pan)	<i>rosina</i>	<i>cydno</i>	4	0.073 ± 0.005	14.71 <sup>e</sup>	<0.0001	4.4 ± 0.3
<i>melp.</i> (FG)	<i>rosina</i>	<i>cydno</i>	4 + 3 + 2	0.493 ± 0.009	53.08 <sup>e</sup>	<0.0001	27.6 ± 0.8
<i>amaryllis</i>	<i>rosina</i>	<i>cydno</i>	4 + 3 + 2	0.490 ± 0.009	56.83 <sup>e</sup>	<0.0001	29.3 ± 0.8
<i>aglaope</i>	<i>rosina</i>	<i>cydno</i>	4 + 3 + 2	0.501 ± 0.009	55.49 <sup>e</sup>	<0.0001	29.7 ± 0.9
Z chromosome							
<i>aglaope</i>	<i>amaryllis</i>	<i>timareta</i>	4	0.092 ± 0.098	0.94	0.3460	1.1 ± 1.1
<i>melp.</i> (FG)	<i>amaryllis</i>	<i>timareta</i>	4 + 3	0.204 ± 0.074	2.77 <sup>f</sup>	0.0056	2.5 ± 1.1
<i>rosina</i>	<i>amaryllis</i>	<i>timareta</i>	4 + 3 + 2	0.140 ± 0.057	2.47 <sup>g</sup>	0.0136	2.2 ± 1.1
<i>melp.</i> (Pan)	<i>amaryllis</i>	<i>timareta</i>	4 + 3 + 2	0.155 ± 0.059	2.64 <sup>f</sup>	0.0082	2.4 ± 1.1
<i>melp.</i> (Pan)	<i>rosina</i>	<i>cydno</i>	4	0.050 ± 0.012	4.27 <sup>e</sup>	<0.0001	0.7 ± 0.2
<i>melp.</i> (FG)	<i>rosina</i>	<i>cydno</i>	4 + 3 + 2	0.191 ± 0.025	7.52 <sup>e</sup>	<0.0001	4.0 ± 0.8
<i>amaryllis</i>	<i>rosina</i>	<i>cydno</i>	4 + 3 + 2	0.103 ± 0.008	12.46 <sup>e</sup>	<0.0001	2.3 ± 0.4
<i>aglaope</i>	<i>rosina</i>	<i>cydno</i>	4 + 3 + 2	0.120 ± 0.030	3.94 <sup>f</sup>	0.0001	2.7 ± 0.9

P<sub>1</sub>, P<sub>2</sub>, and P<sub>3</sub> refer to the three populations used for the ABBA BABA tests (see Methods for details). (*aglaope*) *H. m. aglaope*; (*amaryllis*) *H. m. amaryllis*; (*rosina*) *H. m. rosina*; (*melp.*) *H. m. melpomene*; (*cydno*) *H. c. chioneus*; (*timareta*) *H. t. thelxinoe*; (Pan) Panama; (FG) French Guiana.

<sup>a</sup>Period over which gene flow is measured, as shown in Figure 3A.

<sup>b</sup>D statistic, to test for an overrepresentation of ABBA versus BABA patterns, ± standard error.

<sup>c</sup>Z-score and P-value for the block jack-knife test of whether D differs significantly from zero.

<sup>d</sup>Estimated fraction of introgression, given as a percentage ± standard error.

<sup>e</sup>Indicates D significantly different from 0, *P* < 0.0001.

<sup>f</sup>Indicates D significantly different from 0, *P* < 0.01.

<sup>g</sup>Indicates D significantly different from 0, *P* < 0.05.

pears to have been shared more anciently, giving sufficient time for introgressed haplotypes to be broken down. Similar differences were observed in the extent of LD among variants shared between *H. cydno* and *H. m. rosina* at the two time intervals examined. By exploiting a different aspect of the data, these results provide an independent line of evidence that both recent and ancient admixture has occurred between these species pairs.

### Patterns of genomic divergence along the speciation continuum

We characterized patterns of divergence across the genome between populations at various levels of divergence and geographic separation using the fixation index, *F*<sub>ST</sub>. At the earliest stage of divergence, between parapatric races, *F*<sub>ST</sub> was low throughout the genome with just a few narrow peaks (Fig. 4), which are partly explained by known wing pattern divergence. Between *H. m. aglaope* and *H. m. amaryllis* from Peru, only two pronounced divergence peaks were present, corresponding to the known pattern loci *HmB* (red elements) and *HmYb* (yellow elements) (Baxter et al. 2010; Nadeau et al. 2012). For the Panamanian races, the level of *F*<sub>ST</sub> was noisier but there was a small *F*<sub>ST</sub> peak at the *HmYb* locus (Fig. 4). There was no peak at the *HmB* locus, consistent with the fact that the Panamanian races share the same red mimetic patterns. Between allopatric races, background *F*<sub>ST</sub> was significantly higher and more heterogeneous, and color pattern loci no longer appeared as clear outliers. Patterns of *F*<sub>ST</sub> between species were broadly similar in mean and variance to those between allopatric races of *H. melpomene* (Figs. 4, 5).

### Reduced interspecific divergence in sympatry

Gene flow between sympatric populations should lead to reduced *F*<sub>ST</sub> as compared with that between allopatric populations. Con-

sistent with phylogenetic evidence for gene flow in sympatry, *F*<sub>ST</sub> between sympatric species pairs in both Panama and Peru was significantly lower than that between either *H. timareta* or *H. cydno* and the allopatric *H. m. melpomene* from French Guiana (Table 3). Each of the 21 chromosomes independently showed the same trend of significantly lower *F*<sub>ST</sub> in sympatry than in allopatry (Supplemental Fig. S5B). This trend is also robust to the use of different allopatric populations. Peruvian *H. m. amaryllis* can be considered as allopatric to Panamanian *H. cydno* (separated by the Andes). Likewise, *H. m. rosina* can be considered allopatric to *H. timareta*. These allopatric comparisons both displayed significantly higher average *F*<sub>ST</sub> than the sympatric comparisons, although not quite as high as when the French Guianan population was used (Supplemental Table S3). This variation may be partly due to differences in the extent of isolation, but probably also reflect differences in effective population size. Nevertheless no inter-species allopatric comparison showed anything close to the reduced *F*<sub>ST</sub> observed between the species in sympatry (Fig. 5).

Plotted across individual chromosomes, the pattern of *F*<sub>ST</sub> was highly heterogeneous in both sympatry and allopatry (Supplemental Figs. S5C, S6, S7). As admixture between species is expected to be non-uniformly distributed across the genome, we predicted that there would be greater heterogeneity in *F*<sub>ST</sub> in sympatry. Indeed the coefficient of variation was significantly greater for *F*<sub>ST</sub> between sympatric pairs than allopatric pairs (Table 3).

Comparison of *F*<sub>ST</sub> in sympatry relative to that in allopatry may be useful in identifying regions subject to divergent selection and hence reduced gene flow. When plotted across individual chromosomes, the trend of lower *F*<sub>ST</sub> in sympatry was widespread but punctuated by narrow regions at which *F*<sub>ST</sub> between the sympatric populations approached and occasionally exceeded that between allopatric populations (Supplemental Figs. S5C, S6, S7). Assuming that the allopatric population pair provides a reference

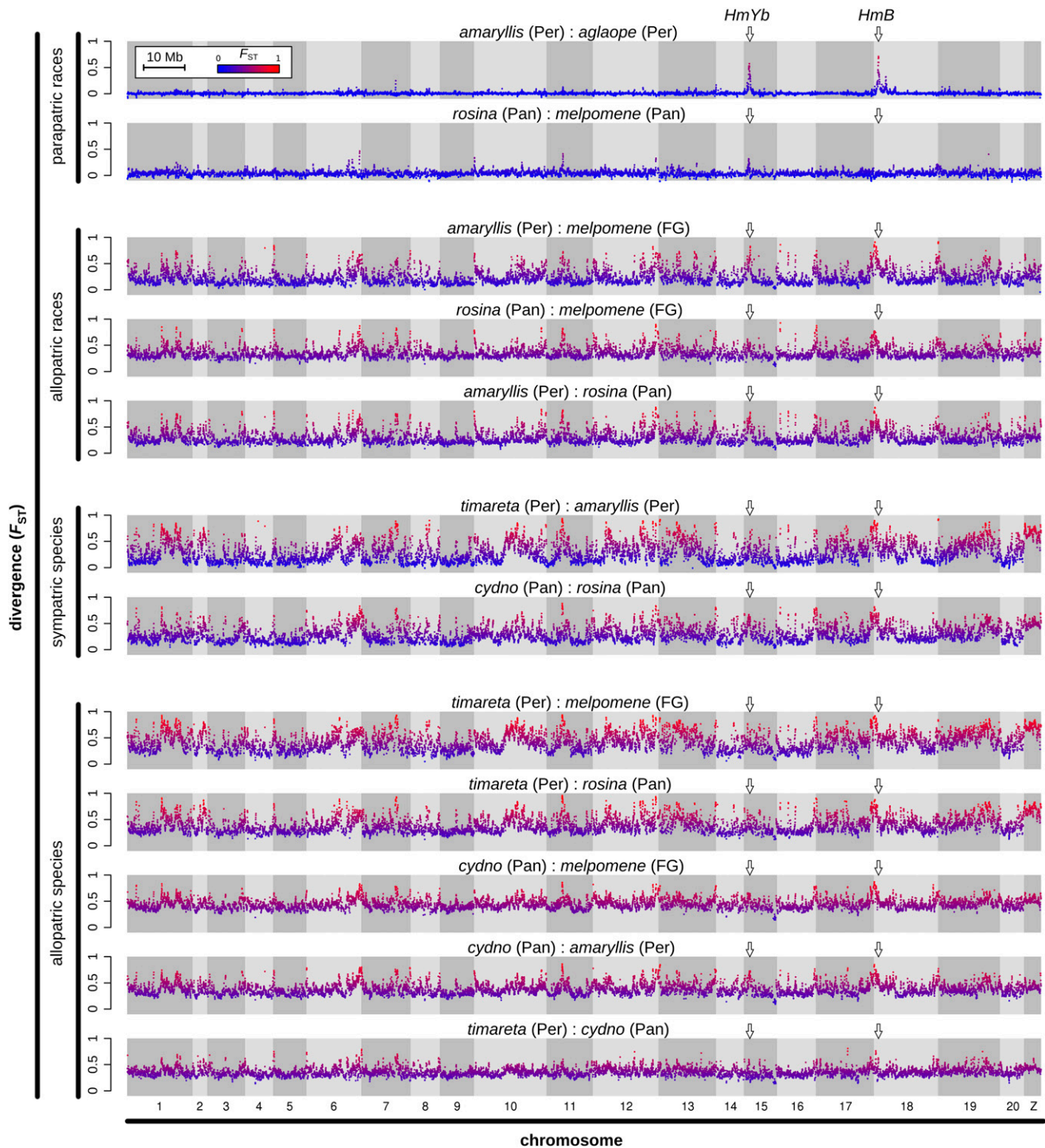


**Figure 4.** Genomic divergence along the speciation continuum.  $F_{ST}$  values were calculated for 100-kb windows sliding in increments of 20 kb. Chromosomes are shown with alternating light and dark shading. Point colors reflect the absolute level of  $F_{ST}$  to allow for comparison between plots. The locations of the wing pattern loci *HmYb* and *HmB* are indicated by arrows. (*amaryllis*) *H. m. amaryllis*; (*rosina*) *H. m. rosina*; (*melpomene*) *H. m. melpomene*; (*cydno*) *H. c. chioneus*; (*timareta*) *H. t. thelxinoe*; (Pan) Panama; (Per) Peru; (FG) French Guiana.

for expected  $F_{ST}$  in the absence of gene flow, these regions indicate putative loci at which selection has acted to eliminate introgressed alleles. This hypothesis is supported by the wing pattern loci. *H. cydno* and *H. m. rosina* have divergent color patterns, and  $F_{ST}$  at both the *HmB* and *HmYb* patterning loci was similar in sympatry

and allopatry (Supplemental Fig. SSC). In contrast, between *H. timareta* and *H. m. amaryllis*, which have convergent wing patterns due to recent introgression (The *Heliconius* Genome Consortium 2012; Pardo-Diaz et al. 2012), there were narrow regions of reduced  $F_{ST}$  between the sympatric pair at both patterning loci.



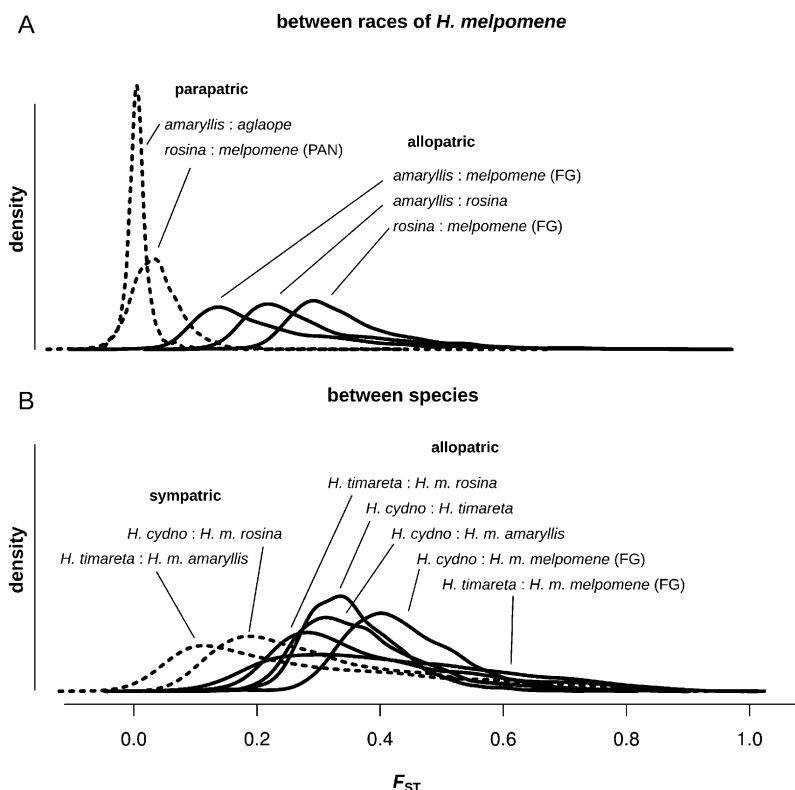


**Figure 5.** Density plots of pairwise  $F_{ST}$  values for non-overlapping 100-kb windows. All pairwise comparisons, corresponding to the plots in Figure 4, between races of *H. melpomene* (A), and between species (B).

### Enhanced reproductive isolation of the Z chromosome

Multiple lines of evidence suggest that gene flow has been reduced throughout the Z chromosome compared with the rest of the genome. Estimates of the fraction of introgression for the Z chromosome were strikingly reduced compared with genome-wide estimates (Fig. 3C; Table 2). In fact, there is no evidence for significant recent Z chromosomal admixture between *H. timareta* and *H. m. amaryllis* (Tables 1, 2).

Patterns of genomic differentiation were also consistent with reduced gene flow across the Z chromosome. For most population pairs, the Z chromosome had a significantly elevated level of  $F_{ST}$  compared with autosomes (Supplemental Table S3; Supplemental Fig. S5B,C). Higher  $F_{ST}$  on this chromosome compared with autosomes is expected given its lower effective population size. However, the ratio of sympatric/allopatric  $F_{ST}$  was closer to one on the Z chromosome ( $\sim 0.9$ ) than on autosomes ( $\sim 0.65$ ) (Table 3). This further supports the hypothesis that admixture on the Z is significantly reduced compared with that on autosomes.

### Discussion

The dominant paradigm among evolutionary biologists has recently shifted from widespread belief in the virtually universal importance of allopatric speciation toward increasing acceptance that

speciation may occur in the presence of some gene flow. However, despite plenty of evidence for hybridization and gene flow between good species, we remain largely ignorant of the extent to which speciation involves ongoing gene flow, both across the genome and through time. If gene flow is indeed common and persistent, then theoretical models of sympatric speciation might be very widely applicable, justifying the recent shift in emphasis (Wu 2001; Pinho and Hey 2010; Smadja and Butlin 2011; Feder et al. 2012). Using whole-genome resequencing combined with structured geographic sampling we now have much greater power to answer these questions. Our data indicate strong signals of admixture between species across a surprisingly large fraction of the genome. This has occurred either continuously or during multiple periods since their initial divergence. Taken together, our results indicate that species divergence can occur in the face of persistent and genome-wide admixture over long periods of time.

### Quantifying gene flow through time

It has long been recognized that both incomplete lineage sorting and hybridization can lead to discordant genealogical histories across the genome. By using

an allopatric population of *Heliconius melpomene* from French Guiana for comparison, we provide evidence that 20%–40% of the genome in *H. melpomene* shows admixture with *H. cydno* or *H. timareta* in sympatry. The window-based phylogenetic approach, using 100-kb regions, averages over large numbers of sites but ensures that each 100-kb tree is statistically well-supported. Furthermore, this result was highly robust to variation in window size.

We extended the site-based ABBA/BABA method to quantify gene flow through time. A previous analysis of *H. melpomene* and *H. timareta* indicated that  $\sim 2\%$ – $5\%$  of the genome was influenced by gene flow (The *Heliconius* Genome Consortium 2012), but

**Table 3.**  $F_{ST}$  between sympatric and allopatric populations

Population pair	$F_{ST}$ (WG)	$F_{ST}$ (autosomes)	$F_{ST}$ (Z chrom.)	Coeff. var. (WG)
<i>cydno</i> : <i>rosina</i> (sympatric)	0.292 $\pm 0.003$	0.286 $\pm 0.001$	0.515 $\pm 0.004$	0.252 <sup>a</sup>
<i>cydno</i> : <i>melpomene</i> (FG) (allopatric)	0.439 $\pm 0.002^a$	0.440 $\pm 0.001^a$	0.540 $\pm 0.003^a$	0.048
<i>timareta</i> : <i>amaryllis</i> (sympatric)	0.287 $\pm 0.003$	0.282 $\pm 0.002$	0.672 $\pm 0.004$	0.470 <sup>a</sup>
<i>timareta</i> : <i>melpomene</i> (FG) (allopatric)	0.419 $\pm 0.003^a$	0.415 $\pm 0.002^a$	0.716 $\pm 0.004^a$	0.175

Mean  $F_{ST}$  for all non-overlapping 100-kb windows is presented,  $\pm$  standard error. The coefficient of variation is a standardized measure, representing the standard deviation divided by the mean. (*amaryllis*) *H. m. amaryllis*; (*rosina*) *H. m. rosina*; (*melpomene*) *H. m. melpomene*; (*cydno*) *H. c. chioneus*; (*timareta*) *H. t. thelxinoe*; (FG) French Guiana.

<sup>a</sup>Indicates significantly greater  $F_{ST}$  in allopatry (t-test on arcsine square-root transformed values,  $P < 0.0001$ ), and significantly greater coefficient of variation in sympatry (F-test,  $P < 0.001$ ).

this comparison could detect admixture that occurred only over a short, recent time period. Our sampling design here allowed us to vary the choice of ingroup populations and examine gene flow over different time scales. Estimates of admixture increased with increasing length of the time period examined, implying continued gene flow during speciation as opposed to a recent burst. Furthermore, LD between derived alleles that were shared during the recent time period was strongest, indicating the existence of introgressed haplotype blocks that are yet to be broken down fully by recombination. This signal was most extensive for alleles shared between *H. timareta* and *H. m. amaryllis* but absent from *H. m. aglaope*, with LD extending up to 1 Mb. This is consistent with extremely recent gene flow, as *H. m. amaryllis* and *H. m. aglaope* coalesce very recently. In contrast, LD between variants shared over longer time periods was weaker and declined with physical distance at a rate similar to the genome-wide average, implying that most of these admixed variants were shared very long ago. Thus two independent lines of evidence suggest that gene flow extends from early in speciation to the present. While we cannot rule out periods of allopatry during this time, particularly very early during the species divergence, our results imply that admixture has been a major influence on the genome throughout most of the speciation process.

### Genomic divergence through time and space

There has been mixed support for the verbal model of islands of divergence amidst a sea of gene flow (Noor and Bennett 2009; Nosil et al. 2009; Feder et al. 2012). Here we examined this model by comparing patterns of genomic divergence at different stages of speciation and different levels of geographical separation. Parapatric races that are known to hybridize in nature, and in particular *H. m. amaryllis* and *H. m. aglaope* from Peru, displayed patterns of differentiation strongly congruent with this islands of divergence model, with strong differentiation at known wing patterning loci. Nonetheless, patterns of divergence are likely to be heterogeneous regardless of gene flow (Noor and Bennett 2009; Michel et al. 2010). For example, between allopatric populations of *H. melpomene*, subject to isolation by distance and biogeographic barriers such as the Andes, there is a higher average  $F_{ST}$  but also considerable heterogeneity across the genome, including divergence peaks at the color pattern loci. This probably reflects the fact that strong selection, and various other demographic factors, can cause localized reductions in effective population size, such that certain regions appear as outliers for population differentiation, even in the absence of homogenizing gene flow at other loci (Charlesworth 1998; Turner and Hahn 2010). The presence of  $F_{ST}$  outliers alone does not provide sufficient evidence that divergence occurred with ongoing gene flow.

$F_{ST}$  between sympatric species was highly heterogeneous, and was not congruent with an idealized scenario of islands of divergence against an otherwise homogenized genome. Nevertheless, interspecific  $F_{ST}$  between sympatric species was generally lower, and more variable (Table 3) than between the corresponding allopatric populations, as expected under a model of admixture with variable selection against introgressing alleles. The trend of lower  $F_{ST}$  in sympatry was widespread across all chromosomes, consistent with pervasive admixture across the whole genome. Despite this widespread signal, the rate of effective gene flow between *H. melpomene* and the *H. cydno/timareta* clade is apparently insufficient to completely abolish differentiation across most of the genome (Nosil et al. 2009; Feder et al. 2012).

Comparisons of sympatric and allopatric populations also permit detection of outlier loci using the joint distribution of  $F_{ST}$  in sympatry and allopatry. Loci at which interspecific  $F_{ST}$  is similar in sympatry and allopatry could indicate putative targets of divergent selection where the effective rate of gene flow is reduced. In effect, the allopatric population provides a reference for the expected divergence value in the absence of gene flow, controlling for the inherent heterogeneity in rates of divergence across the genome. This is conceptually similar to an approach applied in hybrid zones, where allopatric populations are used as a control to detect introgressed loci (Gompert and Buerkle 2010). Loci known to be under selection offer a test of this logic. *H. cydno* and *H. melpomene* from Panama have distinct wing patterns and both the *HmB* and *HmYb* pattern loci fall under peaks at which  $F_{ST}$  is similar in sympatry and allopatry. The Peruvian pair has convergent wing patterns, and narrow tracts of the genome have here introgressed at both color pattern loci (The *Heliconius* Genome Consortium 2012; Pardo-Diaz et al. 2012). Indeed, at both loci, there is a narrow trough of low  $F_{ST}$  between these populations. The relatively high levels of  $F_{ST}$  surrounding these troughs may be remnants of hitchhiking following initial divergence in wing pattern. Although we are here mostly interested in the genome-wide patterns of divergence and admixture, we believe that in the future such joint distributions of  $F_{ST}$  are likely to provide a powerful method for detection of genomic regions subject to selection.

### The Z chromosome is at a more advanced stage of speciation

There is both theoretical and empirical evidence for a disproportionate role of the sex chromosomes in speciation (Qvarnström and Bailey 2009). Sex-linked genes are expected to diverge more rapidly (Coyne and Orr 2004), and in the Lepidoptera species differences have been shown to map disproportionately to the Z chromosome (Prowell 1998). In our data there was a significantly reduced signal of admixture on the Z chromosome compared with autosomes. The discrepancy between the Z and autosomal  $F_{ST}$  was also considerably greater in sympatry than in allopatry (Table 3). Thus the difference cannot be explained solely by reduced effective population size of sex chromosomes. Numbers of shared derived alleles suggest that ancient gene flow did occur on the Z, but that the contemporary migration rate for this chromosome is very low. This can be explained, in part, by Z-autosome incompatibilities known to cause female hybrid sterility (Jiggins et al. 2001; Naisbit et al. 2002). These sex chromosome versus autosome patterns are similar to those seen in the genomes of the *Drosophila simulans* group and in *Ficedula* flycatchers (Ellegren et al. 2012; Garrigan et al. 2012), providing general support for the hypothesis that sex chromosomes play a major role in speciation.

### Conclusions

Genomic methods offer the opportunity to address the ongoing debate between recent proponents of sympatric speciation and the classical wisdom of ubiquitous allopatric speciation. It is unlikely that genomic data from extant species will ever rule out brief periods of allopatry during speciation. Nonetheless, it is clear from our results that admixture between *H. melpomene* and the *H. cydno/timareta* lineage has taken place on a large scale throughout much of their divergence history. To some extent, our findings fit with verbal ideas of speciation with gene flow (Wu 2001; Feder et al. 2012), in which a progression from narrow islands leads to more genomically widespread divergence. Indeed, despite increasing

genome-wide divergence later on, the effects of gene flow remain pervasive throughout the genome. Up to 40% of the genome shows a discordant phylogenetic pattern consistent with admixture in sympatry. Our results imply that the recent focus on mechanisms that permit speciation-with-gene-flow in the literature is not misguided (Servedio et al. 2011; Smadja and Butlin 2011). In the case of *H. melpomene* and *H. cydno*, wing patterns have a relatively simple genetic basis (Naisbit et al. 2007), and the loci that affect male mate preference and hybrid sterility are associated with color pattern loci (Merrill et al. 2011b), both of which should make speciation easier. Genomics therefore has provided empirical data that help answer thorny questions about the relative importance of allopatric isolation in speciation, which have hitherto proved to be among the most intractable debates in evolutionary biology.

## Methods

### Whole-genome resequencing and genotype calling

Samples were preserved in NaCl-saturated DMSO solution at  $-20^{\circ}\text{C}$  and DNA was isolated using the DNeasy Blood and Tissue Kit (Qiagen). Illumina paired-end libraries were generated according to the manufacturer's protocol (Illumina Inc.). These were shotgun sequenced on either Illumina's Genome Analyzer IIx system or Illumina's HiSeq 2000 system, according to the manufacturer's protocol (Illumina Inc.).

Quality-filtered, paired-end sequence reads were mapped to the *H. melpomene* genome scaffolds (version 1.1) (The *Heliconius* Genome Consortium 2012) using Stampy v1.0.13 (Lunter and Goodson 2011). Defaults were used for all parameters with the exception of the expected substitution rate, which was set to 0.03 for *H. melpomene* samples (0.001 for the individual from the reference genome strain), 0.04 for *H. cydno/timareta* samples, and 0.05 for outgroup silvaniform samples to allow mapping of reads from divergent species. To minimize false SNPs due to inconsistent mapping around indels, base alignment quality (BAQ) was considered during mapping, and then local realignment around indels was performed using the Genome Analysis Tool Kit (GATK) v1.6 (DePristo et al. 2011). SAM/BAM file conversion, analysis, and filtering were performed using SAMtools (Li et al. 2009) and Picard (<http://picard.sourceforge.net>). PCR-duplicate reads were removed using Picard.

Genotypes were called using the GATK v1.6 UnifiedGenotyper (DePristo et al. 2011). Individuals from the same population were genotyped simultaneously. Default parameters were used, except expected heterozygosity was set to 0.01, and BAQ calculation was performed where necessary to optimize calls around indels. For a genotype call to be considered high quality, it had to meet the following criteria: Quality (QUAL)  $\geq 30$ ,  $10 \leq \text{depth} \leq 200$  (the upper bound was imposed to avoid false SNPs due to mis-mapping in repetitive regions), and for variant (non-reference) calls, genotype quality (GQ)  $\geq 30$ . Only these "high-quality" genotype calls were used in downstream analyses. Genotyping summary statistics for each sample are provided in Supplemental Table S1.

### Assigning scaffolds to chromosomes

Several analyses involved comparisons among chromosomes. Scaffolds were assigned to chromosomes based on the *Heliconius melpomene* linkage map (The *Heliconius* Genome Consortium 2012), version 1.1, which has  $\sim 80\%$  of the genome assigned to chromosomes. An important focus of this study was the comparison between autosomal and Z-linked regions. We therefore performed extra tests to confirm Z-linkage of mapped scaffolds and

identify additional Z-linked scaffolds among those previously unmapped (see Supplemental Appendix A for details). This procedure also identified several mis-assembled scaffolds that were Z/autosomal chimeras. Using the most likely breakpoints identified, we removed Z-linked regions from autosomes and also removed autosomal regions from the Z-linked scaffolds.

### Phylogenomic analysis

A whole-genome ML tree was generated using only sites in the genome with high-quality genotype calls for all 31 individuals, resulting in an alignment of 60 Mb. RAXML (Stamatakis 2006; Ott et al. 2007; Stamatakis et al. 2008) was used with the GTRGAMMA model, and 100 bootstrap replicates were performed. A separate tree was constructed for the mitochondrial genome (alignment of 9.5 kb), using the same procedure, but with 1000 bootstraps. To investigate phylogenetic discordance across the genome, independent ML trees were generated for non-overlapping 100-kb windows. To minimize artifacts of data quality, only sites with a high-quality genotype call for all 31 genomes were used, and windows that contained  $<10000$  sites were rejected.

### Four-population tests for admixture

To test for admixture between pairs of heterospecific populations, we used the four-population test (Reich et al. 2009, 2012). This test is based on the fact that genetic drift should be uncorrelated in unadmixed populations. Given the populations A, B, C, and D, with the unrooted relationship [(A,B),(C,D)], the  $f_4$  statistic,  $f_4(A,B;C,D)$ , allows a test for whether allele frequency differences between A and B are correlated with differences between C and D, thus indicative of admixture (either between A and C, or between B and D, or both). We calculated the  $f_4$  statistic (Equation S6.1 of Reich et al. 2012) using all informative sites, i.e., biallelic sites at which both pairs of populations differ in allele frequency. The mean and variance in  $f_4$  were then estimated using a block jackknifing approach (Reich et al. 2009), which controls for LD among sites. We used a block size of 1 Mb, far greater than the extent of LD in the *Heliconius* genomes studied here (Supplemental Fig. S2; The *Heliconius* Genome Consortium 2012). This allowed us to test whether  $f_4$  deviated significantly from zero. Such deviations would indicate that the allele frequency differences between the two population pairs are significantly correlated, indicating gene flow.

### Quantifying gene flow over specific time periods

To quantify gene flow along a specific branch of the phylogeny, we used a method based on the relative abundance of two classes of polymorphic sites called "ABBAs" and "BABAs" (Green et al. 2010; Durand et al. 2011). Given four populations,  $P_1$ ,  $P_2$ ,  $P_3$ , and an outgroup O, with the relationship  $\{[(P_1,P_2),P_3],O\}$ , ABBAs are SNPs at which  $P_2$  and  $P_3$  share a derived allele "B," while  $P_1$  retains the ancestral allele "A," as inferred from the outgroup (i.e.,  $P_2 = P_3 \neq P_1 = O$ ). Similarly, BABAs are SNPs at which  $P_1$  and  $P_3$  share a derived allele "B," while  $P_2$  retains the ancestral allele "A" (i.e.,  $P_1 = P_3 \neq P_2 = O$ ). Under the null hypothesis of no gene flow, ABBA and BABA patterns can only arise via incomplete lineage sorting, and should be equally infrequent (assuming no recurrent mutation and random mating in the ancestral population). However, if there has been gene flow between  $P_3$  and  $P_2$  since the split between  $P_1$  and  $P_2$ , there should be an overrepresentation of ABBA patterns. The relative abundance of ABBA and BABA patterns throughout the genome was compared using the  $D$  statistic (Equation 2 of Durand et al. 2011), based on allele frequencies at each SNP. Only sites at which the four outgroup genomes were homozygous for

the same allele were considered to ensure confident assignment of the ancestral and derived states. We used a 1-Mb block jack-knifing approach to calculate the mean and variance of  $D$ , allowing a test for whether  $D$  differed significantly from zero.

We then estimated  $f$ , the fraction of the genome that is admixed. In the example described above, the fraction of the genome that is admixed between  $P_3$  and  $P_2$  subsequent to the split between  $P_1$  and  $P_2$  can be estimated by comparing the observed difference in abundance of ABBA and BABA patterns with that which would be expected under a scenario of 100% admixture between  $P_3$  and  $P_2$  (Equation 8 of Durand et al. 2011). As above, we used a 1-Mb block jack-knife approach to calculate the mean and variance of the  $f$  value.

### Estimating the extent of linkage disequilibrium (LD)

Linkage disequilibrium (LD) was estimated using all pairs of biallelic sites with high-quality genotype calls in all 31 genomes and a minor allele count of at least five. We estimated  $r^2$  within *H. melpomene* populations using the ML estimator (Clayton and Leung 2007), implemented in the R package “snpstats,” which does not require phased haplotypes. To investigate how LD breaks down with distance,  $r^2$  values were binned according to distance in logarithmically increasing bin sizes, to account for small numbers of SNP pairs at large distances. Only SNP pairs on the same scaffold were considered. To obtain an estimate of background LD between unlinked sites, subsets of 500 SNPs were randomly selected and  $r^2$  was estimated for all pairs for which the two SNPs were on separate chromosomes. This procedure was repeated 100 times and a 95% confidence interval was calculated.

We investigated the rate of decline in LD between shared derived alleles in *H. m. amaryllis* and *H. m. rosina*. Following the definition of an ABBA site above, all sites at which  $P_1$  was fixed for the ancestral state while  $P_2$  and  $P_3$  carried a derived allele were considered.  $r^2$  values were binned according to distance as described above.

### Patterns of genetic differentiation between populations

We estimated levels of genetic differentiation between populations by calculating  $F_{ST}$  for 100-kb genomic windows. Nadeau et al. (2012) showed that averaging over large numbers of sites in this way provides highly repeatable  $F_{ST}$  estimates from small samples.  $F_{ST}$  was calculated using the EggLib Python module (De Mita and Siol 2012). To minimize variation due to stochasticity and genotyping errors, windows were rejected if they contained <2500 variant sites genotyped with high quality for all individuals from the two populations being analyzed. Windows were restricted to single scaffolds (i.e., they did not cross scaffold boundaries). To plot  $F_{ST}$  across chromosomes, scaffolds were arranged according to the *H. melpomene* linkage map (The *Heliconius* Genome Consortium 2012), version 1.1, having corrected for the several Z/autosome chimeric scaffolds identified as described in Supplemental Appendix A.

### Data access

Whole-genome shotgun sequencing paired-end FASTQ files have been submitted to the European Nucleotide Archive (ENA; <http://www.ebi.ac.uk/ena/>) under accession number ERP002440. The following files have been deposited in the Data Dryad repository (<http://datadryad.org/resource/doi:10.5061/dryad.dk712>): all processed VCF files, site-based allele frequency data used for the four-population tests and ABBA BABA analyses, all pairwise  $F_{ST}$  values for 100-kb windows, maximum-likelihood trees for each

100-kb window for the two four-taxon data sets analyzed (Newick format), data files providing the topology supported by each window, a list of scaffolds and scaffold regions designated as Z-linked, and custom Python and R scripts used for data analyses.

### Acknowledgments

We thank Richard Merrill and Simon Baxter for field work. Judith Mank and Jamie Walters kindly contributed funds from their Fell Fund grant. We also thank Anders Eriksson for his input in discussions of this study. Lastly, we are most grateful to the three anonymous referees, whose thoughtful and in-depth reviews greatly improved the standard of this work. This study was funded by the BBSRC (G006903/1, G008841/1, and H01439X/1), the Leverhulme Trust (F/09364/E), and The Fell Fund.

### References

- Baxter SW, Nadeau NJ, Maroja LS, Wilkinson P, Counterman BA, Dawson A, Beltran M, Perez-Espona S, Chamberlain N, Ferguson L, et al. 2010. Genomic hotspots for adaptation: The population genetics of Müllerian mimicry in the *Heliconius melpomene* clade. *PLoS Genet* **6**: 12.
- Bouckaert RR. 2010. DensiTree: Making sense of sets of phylogenetic trees. *Bioinformatics* **26**: 1372–1373.
- Bull V, Beltrán M, Jiggins CD, McMillan WO, Bermingham E, Mallet J. 2006. Polyphyly and gene flow between non-sibling *Heliconius* species. *BMC Biol* **4**: 11.
- Chamberlain NL, Hill RI, Kapan DD, Gilbert LE, Kronforst MR. 2009. Polymorphic butterfly reveals the missing link in ecological speciation. *Science* **326**: 847–850.
- Charlesworth B. 1998. Measures of divergence between populations and the effect of forces that reduce variability. *Mol Biol Evol* **15**: 538–543.
- Clayton D, Leung H-T. 2007. An R package for analysis of whole-genome association studies. *Hum Hered* **64**: 45–51.
- Coyne JA, Orr HA. 2004. *Speciation*. Sinauer, Sunderland, MA.
- De Mita S, Siol M. 2012. EggLib: Processing, analysis and simulation tools for population genetics and genomics. *BMC Genet* **13**: 27.
- DePristo MA, Banks E, Poplin R, Garimella KV, Maguire JR, Hartl C, Philippakis AA, del Angel G, Rivas MA, Hanna M, et al. 2011. A framework for variation discovery and genotyping using next-generation DNA sequencing data. *Nat Genet* **43**: 491–498.
- Durand EY, Patterson N, Reich D, Slatkin M. 2011. Testing for ancient admixture between closely related populations. *Mol Biol Evol* **28**: 2239–2252.
- Ellegren H, Smeds L, Burri R, Olason PI, Backström N, Kawakami T, Küstner A, Mäkinen H, Nadachowska-Brzyska K, Qvarnström A, et al. 2012. The genomic landscape of species divergence in *Ficedula* flycatchers. *Nature* **491**: 756–760.
- Eriksson A, Manica A. 2012. Effect of ancient population structure on the degree of polymorphism shared between modern human populations and ancient hominins. *Proc Natl Acad Sci* **109**: 13956–13960.
- Feder J, Egan S, Nosil P. 2012. The genomics of speciation-with-gene-flow. *Trends Genet* **28**: 342–350.
- Gagnaire P-A, Pavey SA, Normandeau E, Bernatchez L. 2013. The genetic architecture of reproductive isolation during speciation-with-gene-flow in lake whitefish species pairs assessed by rad-sequencing. *Evolution* **67**: 2483–2497.
- Garrigan D, Kingan SB, Geneva AJ, Andolfatto P, Clark AG, Thornton K, Presgraves DC. 2012. Genome sequencing reveals complex speciation in the *Drosophila simulans* clade. *Genome Res* **22**: 1499–1511.
- Gavrilets S. 2004. *Fitness landscapes and the origin of species*. Princeton University Press, Princeton, NJ.
- Giraldo N, Salazar C, Jiggins CD, Bermingham E, Linares M. 2008. Two sisters in the same dress: *Heliconius* cryptic species. *BMC Evol Biol* **8**: 324.
- Gompert Z, Buerkle AC. 2010. Introgress: A software package for mapping components of isolation in hybrids. *Mol Ecol Resour* **10**: 378–384.
- Grant PR, Grant BR, Petren K. 2005. Hybridization in the recent past. *Am Nat* **166**: 56–67.
- Green RE, Krause J, Briggs AW, Maricic T, Stenzel U, Kircher M, Patterson N, Li H, Zhai W, Fritz MH-Y, et al. 2010. A draft sequence of the Neandertal genome. *Science* **328**: 710–722.
- The *Heliconius* Genome Consortium. 2012. Butterfly genome reveals promiscuous exchange of mimicry adaptations among species. *Nature* **487**: 94–98.
- Hohenlohe PA, Bassham S, Etter PD, Stiffler N, Johnson EA, Cresko WA. 2010. Population genomics of parallel adaptation in threespine stickleback using sequenced RAD tags. *PLoS Genet* **6**: e1000862.

- Hohenlohe PA, Bassham S, Currey M, Cresko WA. 2012. Extensive linkage disequilibrium and parallel adaptive divergence across threespine stickleback genomes. *Philos T Roy Soc B* **367**: 395–408.
- Jiggins C. 2008. Ecological speciation in mimetic butterflies. *Bioscience* **58**: 541–548.
- Jiggins CD, Linares M, Naisbit RE, Salazar C, Yang ZH, Mallet J. 2001. Sex-linked hybrid sterility in a butterfly. *Evolution* **55**: 1631–1638.
- Kirkpatrick M, Ravigné V. 2002. Speciation by natural and sexual selection: Models and experiments. *Am Nat* (Suppl) **159**: S22–S35.
- Kronforst MR, Young LG, Blume LM, Gilbert LE. 2006. Multilocus analyses of admixture and introgression among hybridizing *Heliconius* butterflies. *Evolution* **60**: 1254–1268.
- Kulathinal RJ, Stevison LS, Noor MAF. 2009. The genomics of speciation in *Drosophila*: Diversity, divergence, and introgression estimated using low-coverage genome sequencing. *PLoS Genet* **5**: e1000550.
- Lawnczak MKN, Emrich SJ, Holloway AK, Regier AP, Olson M, White B, Redmond S, Fulton L, Appelbaum E, Godfrey J, et al. 2010. Widespread divergence between incipient *Anopheles gambiae* species revealed by whole genome sequences. *Science* **330**: 512–514.
- Li H, Handsaker B, Wysoker A, Fennell T, Ruan J, Homer N, Marth G, Abecasis G, Durbin R. 2009. The Sequence Alignment/Map format and SAMtools. *Bioinformatics* **25**: 2078–2079.
- Lunter G, Goodson M. 2011. Stampy: A statistical algorithm for sensitive and fast mapping of Illumina sequence reads. *Genome Res* **21**: 936–939.
- Machado CA, Kliman RM, Markert JA, Hey J. 2002. Inferring the history of speciation from multilocus DNA sequence data: The case of *Drosophila pseudoobscura* and close relatives. *Mol Biol Evol* **19**: 472–488.
- Mallet J. 2005. Hybridization as an invasion of the genome. *Trends Ecol Evol* **20**: 229–237.
- Mallet J, Beltrán M, Neukirchen W, Linares M. 2007. Natural hybridization in heliconiine butterflies: The species boundary as a continuum. *BMC Evol Biol* **7**: 28.
- Mérot C, Mavárez J, Evin A, Dasmahapatra KK, Mallet J, Lamas G, Joron M. 2013. Genetic differentiation without mimicry shift in a pair of hybridizing *Heliconius* species (Lepidoptera: Nymphalidae). *Biol J Linn Soc Lond* **109**: 830–847.
- Merrill RM, Gompert Z, Dembeck LM, Kronforst MR, McMillan WO, Jiggins CD. 2011a. Mate preference across the speciation continuum in a clade of mimetic butterflies. *Evolution* **65**: 1489–1500.
- Merrill RM, Van Schooten B, Scott JA, Jiggins CD. 2011b. Pervasive genetic associations between traits causing reproductive isolation in *Heliconius* butterflies. *Proc Roy Sci B* **278**: 511–518.
- Merrill RM, Wallbank RWR, Bull V, Salazar PC, Mallet J, Stevens M, Jiggins CD. 2012. Disruptive ecological selection on a mating cue. *Proc Roy Sci B* **279**: 4907–4913.
- Michel APA, Sim S, Powell THQ, Taylor MS, Nosil P, Feder JL. 2010. Widespread genomic divergence during sympatric speciation. *Proc Natl Acad Sci* **107**: 9724–9729.
- Nadeau NJ, Whibley A, Jones RT, Davey JW, Dasmahapatra KK, Baxter SW, Quail MA, Joron M, Ffrench-Constant RH, Blaxter ML, et al. 2012. Genomic islands of divergence in hybridizing *Heliconius* butterflies identified by large-scale targeted sequencing. *Philos Trans R Soc Lond B Biol Sci* **367**: 343–353.
- Nadeau NJ, Martin SH, Kozak KM, Salazar C, Dasmahapatra KK, Davey JW, Baxter SW, Blaxter ML, Mallet J, Jiggins CD. 2013. Genome-wide patterns of divergence and gene flow across a butterfly radiation. *Mol Ecol* **22**: 814–826.
- Naisbit RE, Jiggins CD, Linares M, Salazar C, Mallet J. 2002. Hybrid sterility, Haldane's rule and speciation in *Heliconius cydno* and *H. melpomene*. *Race* **1526**: 1517–1526.
- Naisbit RE, Jiggins CD, Mallet J. 2007. Mimicry: Developmental genes that contribute to speciation. *Evol Dev* **5**: 269–280.
- Noor MAF, Bennett SM. 2009. Islands of speciation or mirages in the desert? Examining the role of restricted recombination in maintaining species. *Heredity* **103**: 439–444.
- Nosil P, Funk DJ, Ortiz-Barrientos D. 2009. Divergent selection and heterogeneous genomic divergence. *Mol Ecol* **18**: 375–402.
- Nosil P, Gompert Z, Farkas TE, Comeault AA, Feder JL, Buerkle CA, Parchman TL. 2012. Genomic consequences of multiple speciation processes in a stick insect. *Proc Roy Sci B* **279**: 5058–5065.
- Ott M, Zola J, Stamatakis A, Aluru S. 2007. Large-scale maximum likelihood-based phylogenetic analysis on the IBM BlueGene/L. In *Proceedings of the 2007 ACM/IEEE conference on supercomputing, SC '07*. Reno, Nevada.
- Pardo-Díaz C, Salazar C, Baxter SW, Mérot C, Figueiredo-Ready W, Joron M, McMillan WO, Jiggins CD. 2012. Adaptive introgression across species boundaries in *Heliconius* butterflies. *PLoS Genet* **8**: e1002752.
- Pinho C, Hey J. 2010. Divergence with gene flow: Models and data. *Annu Rev Ecol Syst* **41**: 215–230.
- Powell DP. 1998. Sex linkage and speciation in Lepidoptera. In *Endless forms: Species and speciation* (ed. Howard DJ, Berlocher SH), pp. 309–319. Oxford University Press, New York.
- Qvarnström A, Bailey RI. 2009. Speciation through evolution of sex-linked genes. *Heredity* **102**: 4–15.
- Reich D, Thangaraj K, Patterson N, Price AL, Singh L. 2009. Reconstructing Indian population history. *Nature* **461**: 489–494.
- Reich D, Patterson N, Campbell D, Tandon A, Mazieres S, Ray N, Parra MV, Rojas W, Duque C, Mesa N, et al. 2012. Reconstructing Native American population history. *Nature* **488**: 370–374.
- Rieseberg LH. 2009. Evolution: Replacing genes and traits through hybridization. *Curr Biol* **19**: R119–R122.
- Rosser N, Phillimore AB, Huertas B, Willmott KR, Mallet J. 2012. Testing historical explanations for gradients in species richness in heliconiine butterflies of tropical America. *Biol J Linn Soc Lond* **105**: 479–497.
- Salazar C, Jiggins CD, Taylor JE, Kronforst MR, Linares M. 2008. Gene flow and the genealogical history of *Heliconius heurippa*. *BMC Evol Biol* **8**: 132.
- Sankararaman S, Patterson N, Li H, Pääbo S, Reich D. 2012. The date of interbreeding between Neandertals and modern humans. *PLoS Genet* **8**: e1002947.
- Servedio MR, Van Doorn GS, Kopp M, Frame AM, Nosil P. 2011. Magic traits in speciation: “Magic” but not rare? *Trends Ecol Evol* **26**: 389–397.
- Smadja CM, Butlin RK. 2011. A framework for comparing processes of speciation in the presence of gene flow. *Mol Ecol* **20**: 5123–5140.
- Stamatakis A. 2006. RAxML-VI-HPC: Maximum likelihood-based phylogenetic analyses with thousands of taxa and mixed models. *Bioinformatics* **22**: 2688–2690.
- Stamatakis A, Hoover P, Rougemont J. 2008. A rapid bootstrap algorithm for the RAxML Web servers. *Syst Biol* **57**: 758–771.
- Supple MA, Hines HM, Dasmahapatra KK, Lewis JJ, Nielsen DM, Lavoie C, Ray DA, Salazar C, McMillan WO, Counterman BA. 2013. Genomic architecture of adaptive color pattern divergence and convergence in *Heliconius* butterflies. *Genome Res* **23**: 1248–1257.
- Turner TL, Hahn MW. 2010. Genomic islands of speciation or genomic islands and speciation? *Mol Ecol* **19**: 848–850.
- Turner TL, Hahn MW, Nuzhdin SV. 2005. Genomic islands of speciation in *Anopheles gambiae*. *PLoS Biol* **3**: e285.
- van Doorn GS, Edelaar P, Weissing FJ. 2009. On the origin of species by natural and sexual selection. *Science* **326**: 1704–1707.
- Wu C. 2001. The genic view of the process of speciation. *Science* **14**: 851–865.

Received April 23, 2013; accepted in revised form August 15, 2013.